J|A|C|S
ARTICLES
Published on Web 02/02/2005

Understanding Structure and Bonding in Early Actinide $6d^05f^0$ MX_6^q (M = Th−Np; X = H, F) Complexes in Comparison with Their Transition Metal $5d^0$ Analogues

Michal Straka,*[,†,§] Peter Hrobárik,[‡] and Martin Kaupp*[,†]

Contribution from the Institut für Anorganische Chemie, Universität Würzburg, Am Hubland, D-97074 Würzburg, Germany, and Institute of Inorganic Chemistry, Slovak Academy of Sciences, Dúbravská cesta 9, SK-84536 Bratislava, Slovakia

Received August 19, 2004; E-mail: straka@mail.uni-wuerzburg.de; kaupp@mail.uni-wuerzburg.de

Abstract: The relationship between structure and bonding in actinide $6d^05f^0$ MX_6^q complexes (M = Th, Pa, U, Np; X = H, F; $q = -2, -1, 0, +1$) has been studied, based on density functional calculations with accurate relativistic actinide pseudopotentials. The detailed comparison of these prototype systems with their $5d^0$ transition metal analogues (M = Hf, Ta, W, Re) reveals in detail how the 5f orbitals modify the structural preferences of the actinide complexes relative to the transition metal systems. Natural bond orbital analyses on the hydride complexes indicate that 5f orbital involvement in σ-bonding favors classical structures based on the octahedron, while d orbital contributions to σ-bonding favor symmetry lowering. The respective roles of f and d orbitals are reversed in the case of π-bonding, as shown for the fluoride complexes.

1. Introduction

The early actinide elements Th−Am, with their 5f shell extending into the bonding region, may be considered the first true f elements in the Periodic Table. The 4f shell of the lanthanides is the first of its kind and therefore compact and corelike. The 5f shell contracts with nuclear charge for the later actinides and also approaches corelike character. Both lanthanides and later actinides show thus a d-element-like "rare-earth" behavior. The most important consequences of 5f orbital involvement in early actinide chemistry are perhaps the existence of actinides in variety of oxidation states (e.g., from +III up to +VIII for Pu[1−3]), a propensity to form bulky complexes with often unusual coordination arrangements unknown for transition metal systems, and a pronounced oxophilicity.

Recently, a symmetry trend was noticed[2] in the molecular structures of isoelectronic $6d^05f^0$ actinide oxide and oxyfluoride complexes. When going from lighter to heavier actinide centers along a given isoelectronic series, the molecular structure changes from less to more symmetric, with addition of an inversion center where stoichiometry allows. Experimentally known and previously discussed examples are the $6d^05f^0$ AnO_2^q and AnO_4^q series (q denotes the overall charge of the complex needed to maintain a $6d^05f^0$ configuration). ThO_2 is a bent C_{2v} system ($\alpha = 122.5°$),[4] while UO_2^{2+} is linear.[5] The computationally characterized PaO_2^+ and NpO_2^{3+} are also linear.[2,6,7] In the AnO_4^q (An = U, Np, Pu) series, UO_4^{2-} is tetrahedral, while NpO_4^- and PuO_4 are planar D_{4h} complexes.[2,7] Changes in structural preferences along isoelectronic series were observed computationally also for AnO_2F^q, $AnO_2F_2^q$, AnF_8^q,[2] and AnO_3^q [8] complexes. This presumably general behavior was explained intuitively by increasing stabilization and bonding contributions of 5f orbitals with relatively unchanged 6d orbitals along the Th−Pu series, combined with different structural influences of f and d orbital bonding contributions.[2,9]

Most theoretical investigations have concentrated on the $6d^05f^0$ AnO_2^q series (An = Th−U).[6,9−11] In ThO_2, 6d orbital bonding contributions maximize covalent bonding in a bent structure, in analogy to the d^0 transition metal MO_2^q (M = V, W, Mo) systems.[12,13] The f orbitals are not as strongly involved in bonding as to force a linear structure. Their overall role is not negligible, however, as can be seen from the O−Th−O angle of 122.5°, which is noticeably larger than the 102°−114° O−M−O angles in d^0 MO_2^q systems (M = V, W, Mo).[9,10] In the heavier members of the AnO_2^q series, the f orbitals contract and stabilize (see above) and thus become appreciably bonding. The precise way in which this favors the linear uranyl and related structures is still a matter of argument.[6,9−11] 5f Orbital

† Universität Würzburg.
‡ Slovak Academy of Sciences.
§ Present address: Department of Chemistry, University of Helsinki, POB 55 (A. I. Virtasen aukio 1), FIN-00014 Helsinki, Finland.

(1) Greenwood, N. N.; Earnshaw, A. *Chemistry of the Elements*; Pergamon: Oxford, 1984; p 1468.
(2) Straka, M.; Dyall, K. G.; Pyykkö, P. *Theor. Chem. Acc.* **2001**, *106*, 393.
(3) Domanov, V. P.; Buklanov, G. V.; Lobanov, Yu. V. *J. Nucl. Sci. Technol.* **2002** (Suppl. 3), 579.
(4) Gabelnick, S. D.; Reedy, G. T.; Chasanov, M. G. *J. Chem. Phys.* **1974**, *60*, 1167.
(5) *Gmelin Handbook of Inorganic Chemistry*; Springer-Verlag: Berlin, 1983; Supplement A6.
(6) Dyall, K. G. *Mol. Phys.* **1999**, *96*, 511 and references therein.
(7) Bolvin, H.; Wahlgren, U.; Gropen, O.; Marsden, C. *J. Phys. Chem. A* **2001**, *105*, 10570 and references therein.
(8) Hrobárik, P.; Straka, M.; Kaupp, M. Unpublished work.
(9) Pyykkö, P.; Laakkonen, L. J.; Tatsumi, K. *J. Am. Chem. Soc.* **1989**, *28*, 1801 and references therein.
(10) Tatsumi, K.; Hoffmann R. *Inorg. Chem.* **1980**, *19*, 2656 and references therein.
(11) Wadt, W. R. *J. Am. Chem. Soc.* **1981**, *103*, 6053.
(12) Pyykkö, P.; Tamm, T. *J. Phys. Chem. A* **1997**, *101*, 8107.
(13) Kaupp, M. *Chem.—Eur. J.* **1999**, *5*, 3631.

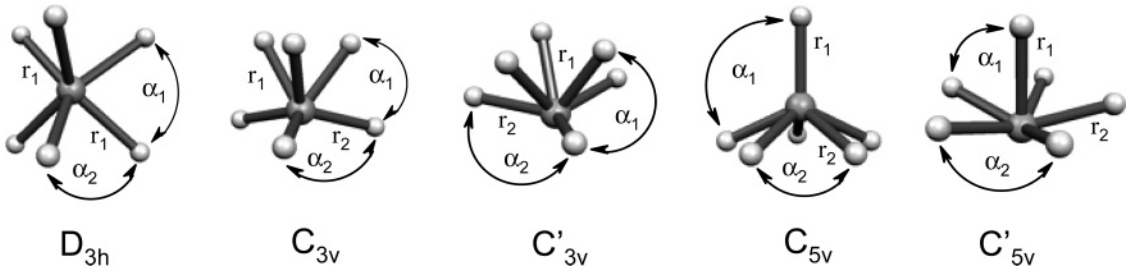

Figure 1. Nonoctahedral MH_6 structures with distance and angle definitions.[16−19]

bonding contributions were also found to be important for the experimentally observed square planar NpO_4^-.[7]

It is instructive to compare the early actinide $6d^05f^0$ systems to their transition metal d^0 analogues. The structures of many of the latter are known to violate the valence-shell electron-pair-repulsion (VSEPR) model, for reasons that have recently been summarized in detail.[14] Examples of such comparisons are the abovementioned MO_2^q species. Another example is UH_6, recently calculated to have an octahedral structure,[15] while the analogous WH_6 is known to prefer C_{3v}, C_{5v}, C_{3v}', and C_{5v}' minima[14,16−18] (cf. Figure 1; matrix isolation IR spectroscopy suggested that the C_{3v} minimum prevails[19]). In the latter case, the "conventional" octahedral structure is only a higher-order stationary point, ca. 400−450 kJ/mol above the minima (see ref 14 for many more examples of non-VSEPR d^0 systems, including $W(CH_3)_6$).

In view of the general importance of hexacoordination in both transition metal and actinide chemistry, we examine here by quantum chemical methods the interrelations between structure and bonding in the prototypical $6d^05f^0$ actinide complexes AnH_6^q (An = Th−U) and AnF_6^q (An = Th−Np), in direct comparison with their transition metal d^0 MH_6^q (M = Hf−W) and MF_6^q (M = Hf−Re) analogues. We aim at a general understanding of interrelations between structural preferences and the involvement of the multitude of different valence orbitals available to an early actinide element. Hydrides and fluorides were chosen as simplest ligands without and with π-bonding, respectively.

2. Computational Methods

All calculations were done with the Gaussian 98 program package,[20] at hybrid density functional level, using the B3LYP functional.[20−22] Convergence criteria *scf* = *tight* (energy and density matrix convergence 10^{-8} au) and integration grid option *grid* = *ultrafine* (99 radial shells and 590 angular points per shell) were used to ensure good numerical accuracy. For the actinides Th, Pa, U, and Np, energy-adjusted relativistic small-core (RSC) pseudopotentials (60 core electrons) were employed, with (12s11p10d8f)/[8s7p6d4f] GTO valence basis sets.[23] For the 5d transition metals Hf, Ta, W, and Re, we used energy-adjusted small-core pseudopotentials (also 60 core electrons) with (8s7p6d)/[6s5p3d] valence basis sets.[24] Spin−orbit coupling is expected to be of minor importance for the structures and energies of the closed-shell species studied here and was neglected. A TZVP all-electron basis was used on H and F atoms.[25] Stationary points on the potential energy surface were characterized by analytical harmonic vibrational frequency analyses. The hybrid DFT methods, pseudopotentials, and basis set levels used have been shown to provide rather accurate structures and energies for both transition metal and actinide systems[14,26] (and were found successful also for ligand NMR chemical shifts in uranium complexes[27]). In particular, we expect that neither the exchange-correlation functional nor basis set or integration accuracy will affect the trends to be discussed.

Bonding was studied by means of Natural Bond Orbital (NBO) and Natural Population Analyses (NPA),[28] using the built-in NBO-3.1 subroutines of the Gaussian 98 program. For the analysis of Natural Localized Molecular Orbitals (NLMO), ionic NBO Lewis structures with one (hydride) or four (fluoride) lone pairs on the ligand were selected (CHOOSE keyword).

All actinide systems studied have formally unoccupied 6d and 5f shell at the ionic limit corresponding to their maximum formal oxidation state. Hence, we were able to perform computational experiments by removing the f functions from the actinide basis set and thereby forcing an actinide to be a "d-only" actinide without f orbitals (assuming that the limited ligand basis set functions cannot compensate for the missing metal f functions). Note that the 4f shell is included in the pseudopotential core and requires thus no basis functions for its description. We could not remove the 6d shell selectively in a similar way by deleting the d basis set, as the 5d shell is treated also as part of the valence shell.

3. Results and Discussion

3.1. Structures and Relative Energies. Hexahydrides. The present calculations (Table 1) confirm that none of the $5d^0$ hexahydrides prefers octahedral structures, as is well docu-

(14) Kaupp, M. *Angew. Chem., Int. Ed. Engl.* **2001**, *40*, 3534 and references therein.
(15) Straka, M.; Patzschke, M.; Pyykkö, P. *Theor. Chem. Acc.* **2003**, *109*, 332.
(16) Kang, S. K.; Tang, H.; Albright, T. A. *J. Am. Chem. Soc.* **1993**, *115*, 1971.
(17) Shen, M.; Schaefer, H. F., III; Partridge, H. *J. Chem. Phys.* **1993**, *98*, 508.
(18) Landis, C. R.; Firman, T. K.; Root, D. M.; Cleveland, T. *J. Am. Chem. Soc.* **1998**, *120*, 1842. Landis, C. R.; Cleveland, T.; Firman, T. K. *J. Am. Chem. Soc.* **1998**, *120*, 2641.
(19) (a) Wang, X.; Andrews, L. *J. Am. Chem. Soc.* **2002**, *124*, 5636. (b) Wang, X.; Andrews, L. *J. Phys. Chem. A* **2002**, *106*, 6720.
(20) Frisch, M. J.; Trucks, G. W.; Schlegel, H. B.; Scuseria, G. E.; Robb, M. A.; Cheeseman, J. R.; Zakrzewski, V. G.; Montgomery, J. A.; R. E. S., Jr.; Burant, J. C.; Dapprich, S.; Millam, J. M.; Daniels, A. D.; Kudin, K. N.; Strain, M. C.; Farkas, O.; Tomasi, J.; Barone, V.; Cossi, M.; Cammi, R.; Mennucci, B.; Pomelli, C.; Adamo, C.; Clifford, S.; Ochterski, J.; Petersson, G. A.; Ayala, P. Y.; Cui, Q.; Morokuma, K.; Malick, D. K.; Rabuck, A. D.; Raghavachari, K.; Foresman, J. B.; Cioslowski, J.; Oritz, J. V.; Baboul, A. G.; Stefanov, B. B.; Lui, G.; Liashenko, A.; Piskorz, P.; Komaromi, I.; Gomperts, R.; Martin, R. L.; Fox, D. J.; Keith, T.; Al-Laham, M. A.; Peng, C. Y.; Nanayakkara, A.; Gonzalez, C.; Challacombe, M.; Gill, P. M. W.; Johnson, B. G.; Chen, W.; Wong, M. W.; Andres, J. L.; Head-Gordon, M.; Replogle, E. S.; Pople, J. A. *Gaussian 98*; Gaussian, Inc.: Pittsburgh, PA, 1998.
(21) Becke, A. D. *J. Chem. Phys.* **1993**, *98*, 5648.
(22) (a) Lee, C.; Yang, W.; Parr, G. R. *Phys. Rev. B* **1988**, *37*, 785. (b) Miehlich B.; Savin, A.; Stoll, H.; Preuss, H. *Chem. Phys. Lett.* **1989**, *157*, 200.
(23) Küchle, W.; Dolg, M.; Stoll, H.; Preuss, H. *J. Chem. Phys.* **1994**, *100*, 7535.
(24) Andrae, D.; Haeussermann, U.; Dolg, M.; Stoll, H.; Preuss, H. *Theor. Chim. Acta* **1990**, *77*, 123.
(25) Schäfer, A.; Huber, C.; Ahlrichs, R. J. *J. Chem. Phys.* **1994**, *100*, 5829.
(26) (a) Ismail, N.; Heully, J.-L.; Saue, T.; Daudey, J.-P.; Marsden, C. J. *Chem. Phys. Lett.* **1999**, *300*, 296. (b) Han, Y.-K.; Hirao, K. *J. Chem. Phys.* **2000**, *113*, 7345. (c) Han, Y.-K. *J. Comput. Chem.* **2001**, *22*, 2010. (d) Schreckenbach, G.; Hay, P. J.; Martin, R. L. *J. Comput. Chem.* **1999**, *20*, 70. (e) Hay, P. J.; Martin, R. L. *J. Chem. Phys.* **1998**, *109*, 3875. (f) Gagliardi, L.; Roos, B. O. *Chem. Phys. Lett.* **2000**, *331*, 229. (f) Batista, E. R.; Martin, R. L.; Hay, P. J.; Peralta, J. E.; Scuseria, G. E. *J. Chem. Phys.* **2004**, *121*, 2144. (g) L. Gagliardi *J. Am. Chem. Soc.* **2003**, *125*, 7504.
(27) Straka, M.; Kaupp, M. *Chem. Phys.*, in press.
(28) (a) Reed, A. E.; Weinhold, F. J. *Chem. Phys.* **1985**, *83*, 1736. (b) Reed, A. E.; Curtiss, L. A.; Weinhold, F. *Chem. Rev.* **1988**, *88*, 899.

Table 1. Optimized Structures and Energies (Relative to the Lowest Energy Minimum), and Negative Force Constants for Nonminimum Structures, of MH_6^q (M = Hf−W, Th−U) Complexes[a]

system	structure	r_1[b] (pm)	r_2[b] (pm)	α_1[b] (deg)	α_2[b] (deg)	relative energy (kJ mol^{-1})	|k|[c] (mDyne Å^{-1})
HfH_6^{2-}	O_h	201.3				+9.3	0.0133
	D_{3h}	199.0		76.3	85.8	0.0	
TaH_6^-	O_h	187.8				+170.2	0.5681, 0.3373
	D_{3h}	183.1		75.1	86.7	+8.4	0.0951
	C_{3v}	179.5	184.1	74.0	129.2	0.0	
WH_6	O_h	180.6				+462.5	7.9262
	D_{3h}	173.3		75.4	86.5	+133.2	0.8742
	C_{3v}	167.1	171.5	67.5	113.9	+0.6	
	C_{3v}'	165.6	170.9	68.6	119.2	+49.2	
	C_{5v}	173.4	168.5	114.7	64.6	0.0	
	C_{5v}'	164.2	167.8	66.2	65.0	+87.8	
ThH_6^{2-}	O_h	228.5				+12.6	0.0102
		(234.8)				(+51.9)	(0.0748)
	D_{3h}	225.7		75.1	86.7	0.0	
		(229.4)		(75.0)	(86.8)	(0.0)	
PaH_6^-	O_h	211.8				0.0	
		(217.9)				(+92.1)	(0.1794, 0.0263)
	D_{3h}	212.8		68.7	91.5	+81.9	0.2336
		(213.6)		(74.8)	(87.0)	(0.0)	
UH_6	O_h	195.7				0.0	
		(207.7)				(+649.6)	(7.1741)
	D_{3h}	195.0		48.6	104.2	+19.2	1.8826, 0.0462, 0.0396
		(198.9)		(73.7)	(88.1)	(+183.4)	(1.1067, 0.0527)
	C_{3v}	195.8	194.3	48.4	106.2	+19.1	1.3056, 0.0548
		(190.9)	(194.9)	(66.3)	(114.6)	(+8.9)	
	C_3[d]	195.0	194.3	49.1	140.0	+1.6	0.0927
	C_{3v}'	189.7	192.6	54.0	107.3	+59.0	1.0107, 1.0115
		(189.5)	(194.0)	(66.6)	(118.4)	(+51.1)	
	C_{5v}	200.9	192.2	124.0	58.3	+50.1	0.2146, 0.1227
		(196.7)	(192.2)	(115.4)	(64.2)	(0.0)	
	C_{5v}'	182.4	188.8	59.9	61.1	+113.2	0.2013, 0.1697, 0.0509
		(188.1)	(191.4)	(64.8)	(64.3)	(+71.5)	

[a] Results for "d-only" actinides in parentheses. [b] Cf. Figure 1 for labeling of angles and distances. [c] Absolute values of negative force constants. [d] This stationary point was not located for "d-only" UH_6.

mented in the literature.[14,16−19,29,30] Depending on bond ionicity and various other factors, the preferred minima are regular trigonal prismatic D_{3h} (HfH_6^{2-}) or distorted prismatic C_{3v} (TaH_6^-). Several competitive low-lying minima are known for neutral WH_6. These are C_{3v} strongly distorted trigonal prismatic, C_{5v} pentagonal pyramidal, C_{3v}' strongly distorted octahedral, and C_{5v}' inverted pentagonal pyramidal (see Figure 1), of which the former two are thought to be very close and lowest in energy (computations show barriers between different minima to be low, suggesting fluxional behavior[16,31]). In going from left to right in the series, the deviations from VSEPR structures become more dramatic, and octahedral stationary points become less and less competitive (Table 1).

As shown in Table 1, the actinide $6d^05f^0$ hexahydride species exhibit also a nonuniform behavior that differs, however, from the transition metal (TM) systems. ThH_6^{2-} is D_{3h} trigonal prismatic (cf. HfH_6^{2-}, which has a similar energy difference between octahedron and trigonal prism). In contrast, PaH_6^- and UH_6 prefer octahedral minima, unlike their TM analogues TaH_6^- and WH_6, respectively. Interestingly, the octahedral preference is large for Pa but becomes feeble for UH_6. Indeed, the relative energies in Table 1 suggest the unknown UH_6 to be a fluxional molecule, as there are several nonoctahedral stationary points within 20 kJ mol^{-1} within the octahedral minimum. In particular, a C_3 transition state derived from a distorted trigonal prismatic C_{3v} structure (cf. C_{3v} minimum for WH_6) is only 1.6 kJ mol^{-1} above the octahedral minimum. Unfortunately, UH_6 is unlikely to be observable experimentally, as the barriers for the exothermic[15] dissociation $UH_6 \rightarrow UH_4 + H_2$ are extremely low. In fact, optimizations without symmetry starting from the C_3 transition state lead to immediate elimination of H_2. The short H−H distances (ca. 160 pm) of all prismatic stationary points also suggest instability toward H_2 elimination. Moreover, all stationary points derived from a trigonal prism, as well as the C_{3v}' structure, are triplet-unstable (UH_4 has a triplet ground state). In view of the presumably large spin−orbit coupling between close-lying triplet and singlet states, the present scalar relativistic calculations are then only of limited predictive value when moving away from the octahedral structure.

Once we omit the f functions from the actinide basis set (see Computational Methods), the trends in the resulting "d-only" actinide hexahydrides follow closely those in the TM systems, including their preferences for nonoctahedral structures. A slight difference pertains to "d-only" PaH_6^-: It prefers a regular prism (D_{3h}), whereas the corresponding $5d^0$ TaH_6^- shows a slight distortion to C_{3v} (but with only 8 kJ mol^{-1} additional stabilization). Notably, all relevant structural and energetical trends for "d-only" UH_6 match the trends computed for the TM analogue WH_6 (see also ref 15), including even the slight preference for a pentagonal pyramidal C_{5v} over a C_{3v} structure at the given

(29) Kang, S. K.; Albright, T. A.; Eisenstein, O. *Inorg. Chem.* **1989**, *28*, 1611.
(30) (a) Zyubin, A.; Musaev, D. G.; Charkin, O. P. *Russ. J. Inorg. Chem.* **1992**, *37*, 1214. (b) Musaev, D. G.; Charkin, O. P. *Sov. J. Coord. Chem.* **1989**, *15*, 102.
(31) Tanpipat, N.; Baker, J. *J. Phys. Chem.* **1996**, *100*, 19818.

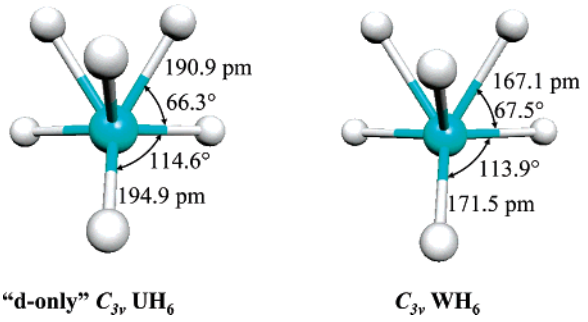

Figure 2. Analogy between structural parameters of C_{3v} minima for "d-only" UH_6 and WH_6.

computational level! Moreover, even the angles and variations of M−H bond lengths for symmetry-nonequivalent positions of the various stationary points are strikingly similar now to those of WH_6 (Table 1; cf. Figure 2 for the C_{3v} minima). All angles agree nicely with those predicted by Landis' valence-bond model for σ-bonded d^0 complexes[18] (see 3.2 below). It can be inferred already at this point that the 5f orbital contributions to bonding must be responsible for most of the differences between actinide $6d^05f^0$ and $5d^0$ hexahydride species (see bonding discussion below).

In all three series, 5d-metals, actinides, and "d-only" actinides, the M−H bond lengths shorten with increasing nuclear charge of the metal center (Table 1). The averaged bond lengths are also shorter in energetically more stable structures of a particular system: for example the average W−H distances in the C_{3v} minimum of WH_6 are shorter than in O_h or D_{3h} structures, whereas octahedral PaH_6^- has shorter distances than its less stable trigonal prismatic structure. This suggests stronger covalent bonds in the more stable structures (small exceptions in Table 1 pertain to some WH_6 and UH_6 structures). In the TM systems, the shorter average distances in distorted structures compared to O_h stationary points are particularly notable. The differences increase along the series, from 1 pm for HfH_6^{2-} to 7 pm for WH_6, when comparing O_h and D_{3h} bond lengths. The opposite trend holds for the actinide systems: the O_h vs D_{3h} An−H bond length difference becomes gradually smaller along the series (the differences range only from about 3 pm in ThH_6^{2-} to 1 pm in UH_6). The bond length trend for the "d-only" actinide series resembles that in the $5d^0$ series. Removal of f functions from the metal basis set increases the An−H bond lengths substantially for ThH_6^{2-} and PaH_6^- and for the UH_6 O_h minimum. In contrast, some U−H bonds shorten in the C_{3v}, C_{3v}', and C_{5v} structures, consistent with their energetic competitiveness for "d-only" UH_6.

Hexafluoride Series. The structural variety of the hexafluoro complexes is much more restricted than that for the hexahydrides. All systems prefer octahedral structures and have trigonal prismatic (D_{3h}) transition states for trigonal twist (Table 2). There appear to be no other low-lying minima or transition states. Notable differences pertain nevertheless to the energetics: The activation barriers for trigonal twist in the $5d^0$ series decrease from about 68 kJ mol^{-1} for HfF_6^{2-} to about 33.4 kJ mol^{-1} for ReF_6^+ (Figure 3), as expected from decreasing ligand repulsion (see lower ligand charges; cf. discussion below) and increasing σ-covalency.[14,29,30] An opposite trend is found for the actinide hexafluoro complexes, with an increase from about 54 kJ mol^{-1} for ThF_6^{2-} to about 123 kJ mol^{-1} for NpF_6^+ (Figure 3). These energetical trends are corroborated by the trends in

Table 2. Optimized Structures and Energies (Relative to the Lowest Energy Minimum), and Negative Force Constants for Nonminimum Structures, of MF_6[q] (M = Hf−Re, Th−Np) Complexes[a]

system	structure	r (pm)	α_1 (deg)	relative energy (kJ mol^{-1})	$\lvert k\rvert$[b] (mDyne $Å^{-1}$)
HfF_6^{2-}	O_h	205.8		0.0	
	D_{3h}	206.4	77.7	+68.4	0.1095
TaF_6^-	O_h	194.2		0.0	
	D_{3h}	194.9	78.1	+67.2	0.1157
WF_6	O_h	186.9		0.0	
	D_{3h}	187.6	78.4	+46.7	0.0684
ReF_6^+	O_h	182.7		0.0	
	D_{3h}	183.5	78.7	+33.4	0.0505
ThF_6^{2-}	O_h	226.9		0.0	
		(233.1)		(0.0)	
	D_{3h}	227.1	77.2	+53.7	0.0778
		(232.5)	(76.7)	(+32.0)	(0.0399)
PaF_6^-	O_h	212.5		0.0	
		(219.7)		(0.0)	
	D_{3h}	213.6	78.3	+80.4	0.1397
		(219.6)	(77.3)	(+47.9)	(0.0719)
UF_6	O_h	201.2		0.0	
		(209.8)		(0.0)	
	D_{3h}	202.4	78.5	+101.8	0.2137
		(209.5)	(77.5)	(+7.3)	(0.0048)
NpF_6^+	O_h	194.6		0.0	
		(204.0)		(+10.0)	
	D_{3h}	196.3	78.8	+123.3	0.2993
		(203.6)	(78.0)	(0.0)	

[a] Results for "d-only" actinides in parentheses. [b] Absolute values of negative force constants.

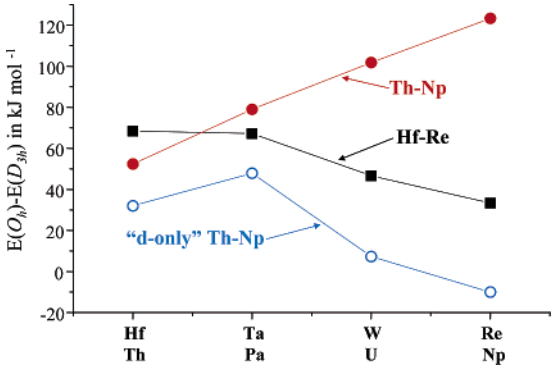

Figure 3. Relative energies of O_h and D_{3h} structures in hexafluoride complexes (positive energies indicate an octahedral preference).

the negative force constants in the D_{3h} transition states (Table 2). Notably, removal of f functions from the actinide basis sets reduces the barriers, in some cases dramatically, and inverts the observed trend in activation barriers completely. It is now similar to that in the TM series (Figure 3). The hypothetical "d-only" NpF_6^+ is even predicted to prefer slightly the trigonal prism over an octahedron, and the energy differences are also very small for "d-only" UF_6. The negative force constants in the D_{3h} transition states are very small in the "d-only" actinide complexes. The decisive role of the 5f shell for differences in structural preferences between the actinide and TM systems is thus again visible already from these calculations with truncated basis sets.

As expected, M−F distances shorten generally along the TM and actinide series, and they are shorter in the octahedral minimum than in the prismatic transition state. In this case, the lengthening of the bonds in the transition state is more pronounced for the actinides than for the TM systems (e.g., 1.7

Table 3. Calculated NPA Charges *q*, Natural Atomic Populations, and Energies of Frontier Orbitals for MH_6^q (M = Hf−W, Th−U) Complexes[a]

system	structure	*q*(M)	*q*(H)[b]	*M*(6p)	metal valence populations s	P	d	f	E_{HOMO} (au)	E_{LUMO} (au)	ΔE[c] (au)
HfH_6^{2-}	O_h	1.77	−0.63		0.62	0.08	1.52	0.00	0.086 40	0.187 46	0.101 06
	D_{3h}	1.34	−0.56		0.59	0.06	2.02	0.00	0.094 84	0.188 18	0.093 34
TaH_6^-	O_h	2.13	−0.52		0.73	0.07	2.06	0.00	−0.096 92	0.030 51	0.127 43
	D_{3h}	1.32	−0.39		0.67	0.04	3.00	0.00	−0.076 99	0.084 33	0.161 32
	C_{3v}	1.06	−0.40		0.66	0.03	3.27	0.00	−0.086 33	0.096 07	0.182 40
			−0.29								
WH_6	O_h	2.41	−0.40		0.87	0.14	2.59	0.00	−0.318 70	−0.265 84	0.052 86
	D_{3h}	1.15	−0.19		0.77	0.05	4.06	0.00	−0.291 75	−0.173 62	0.118 13
	C_{3v}	0.48	−0.15		0.68	0.03	4.85	0.00	−0.309 44	−0.100 83	0.208 61
			−0.01								
	C_{3v}'	0.22	0.06		0.61	0.02	5.20	0.00	−0.296 89	−0.100 69	0.196 20
			−0.13								
	C_{5v}	0.51	−0.20		0.69	0.03	4.82	0.00	−0.302 33	−0.104 47	0.197 86
			−0.06								
	C_{5v}'	−0.06	0.17		0.56	0.01	5.53		−0.277 53	−0.104 43	0.173 10
			−0.02								
ThH_6^{2-}	O_h	2.68	−0.78	5.99	0.58	0.02	0.41	0.32	0.090 99	0.184 16	0.093 17
		(2.72)	(−0.79)	(5.99)	(0.56)	(0.01)	(0.72)	(0.00)	(0.103 83)	(0.185 56)	(0.081 73)
	D_{3h}	2.69	−0.78	5.99	0.53	0.01	0.61	0.18	0.107 72	0.183 00	0.075 28
		(2.72)	(−0.79)	(5.99)	(0.56)	(0.01)	(0.72)	(0.00)	(0.103 83)	(0.185 51)	(0.081 68)
PaH_6^-	O_h	2.41	−0.56	5.93	0.65	0.08	0.27	1.64	−0.090 33	0.043 68	0.134 01
		(3.57)	(−0.76)	(5.99)	(0.75)	(0.05)	(0.63)	(0.00)	(−0.099 57)	(0.051 77)	(0.151 34)
	D_{3h}	2.51	−0.58	5.97	0.56	0.01	0.46	1.49	−0.071 00	0.020 63	0.091 63
		(3.38)	(−0.73)	(5.99)	(0.69)	(0.02)	(0.92)	(0.00)	(−0.082 29)	(0.078 77)	(0.161 06)
UH_6	O_h	2.34	−0.39	5.91	0.73	0.06	0.51	2.44	−0.288 65	−0.162 28	0.126 37
		(3.87)	(−0.65)	(5.99)	(0.81)	(0.05)	(1.27)	(0.00)	(−0.292 54)	(−0.244 73)	(0.047 81)
	D_{3h}	2.52	−0.42	5.94	0.33	0.01	1.00	2.20	−0.229 52	−0.137 66	0.091 86
		(3.05)	(−0.54)	(5.95)	(0.62)	(0.01)	(2.37)	(0.00)	(−0.306 24)	(−0.087 45)	(0.218 79)
	C_{3v}	2.52	−0.42	5.94	0.33	0.01	1.01	2.20	−0.229 86	−0.136 27	0.093 59
			−0.42								
		(3.05)	(−0.47)	(5.95)	(0.62)	(0.01)	(2.37)	(0.00)	(−0.306 11)	(−0.087 50)	(0.218 61)
			(−0.54)								
	C_{3v}'	2.27	−0.36	5.93	0.38	0.01	1.19	2.23	−0.220 28	−0.123 42	0.096 86
			−0.40								
		(2.91)	(−0.44)	(5.94)	(0.60)	(0.01)	(2.54)	(0.00)	(−0.293 31)	(−0.084 40)	(0.208 91)
			(−0.54)								

[a] Results for "d-only" actinides in parentheses. [b] Symmetry-nonequivalent hydrogen positions: Upper value corresponds to r_1, and lower value corresponds to r_2 (cf. Figure 1). [c] HOMO−LUMO gap.

pm for NpF_6^+ compared to 0.8 pm for ReF_6^+). The bond elongation upon removal of f functions from the basis set is large and grows from about 6 pm for ThF_6^{2-} to about 9 pm for NpF_6^+ (Table 2). Interestingly, in the "d-only" actinide series the M−F bond length is slightly shorter for the prism than for the octahedron, opposite to both the TM and "true" actinide series (Table 2).

3.2. Bonding Analyses. Hexahydrides. The bonding trends in d^0 TM systems have been studied extensively during the past decade (see ref 14 and references therein). This holds particularly for systems with exlusively σ-bonds such as the hexahydride complexes, as these exhibit very interesting structures that deviate from VSEPR predictions. Both valence-bond[18] and molecular-orbital[16,32] arguments explain nicely why such "σ-only" d^0 complexes tend to be distorted from VSEPR structures such as the octahedron. For example, the valence-bond model of Landis for WH_6 and related complexes indicates clearly that 67° and 113° angles are preferred by orthogonal sd^5 hybrids rather than the 90° or 180° of an octahedron.[18] This leads naturally to the C_{3v}, C_{3v}', C_{5v}, and C_{5v}' structures shown in Figure 1 (IR spectra in matrix isolation suggest the C_{3v} minimum to be preferred[19]). Similarly, MO symmetry arguments indicate an improved participation of d orbitals in σ-bonding in such lower symmetry structures.[14,16,32,33] It is thus clear that the angular bonding preferences of the metal d orbitals determine to a large extent the structures of these types of TM d^0 complexes.[14] Negative charge tends to concentrate on the ligand and counteracts the distortions (the HOMO−LUMO gap also tends to be larger in these more ionic systems). This explains, for example, why HfH_6^{2-} exhibits a regular prism (D_{3h}) compared to the more strongly distorted WH_6. Our results for the TM hexahydrides are in good agreement with previous studies. NPA charges indicate increasing covalency along the series (Table 3), as well as increased covalency upon distortion to the energetically favorable low-symmetry structures, as discussed before.[14,30] The structural preferences of the "d-only" actinide series obtained here after removal of f functions from the actinide basis sets (cf. Table 1) are almost identical to the $5d^0$ TM series (see above). This indicates that the differences between proper actinide calculations and the TM calculations must arise mainly from the 5f orbital involvement in bonding. In the purely σ-bonded hexahydride series our analyses must thus concentrate on the role the 5f orbitals play in σ-bonding.

NPA metal charges indicate generally more ionic bonding in the An hexahydrides as compared to their TM analogues. The fact that the octahedron is more stabilized for PaH_6^- than

(32) Bayse, C. A.; Hall, M. B. *J. Am. Chem. Soc.* **1999**, *121*, 1348.

(33) King, R. B. *Inorg. Chem.* **1998**, *37*, 3057.

for ThH_6^{2-}, (Table 1), together with the larger metal charges in the "d-only" actinide hydride series (Table 3), provides evidence against ligand repulsion as the main factor stabilizing the octahedron. The metal NPA populations (Table 3) indicate a fast increase of 5f populations along the actinide hexahydride series, similar to previous studies of Mulliken populations along the $6d^05f^5$ AnO_2^q series.[2] This may be understood from the much faster contraction of 5f than 6d orbitals with increasing nuclear charge, which render the 5f shell more and more available for bonding.[9] For example, in ThH_6^{2-} the metal 6d-population exceeds still the 5f population, but the situation reverses for PaH_6^- and UH_6. While both 5f and 6d orbitals play an important role in metal−ligand bonding, the 5f covalency increases along the series. The 6d population remains more or less constant on an absolute scale and thus diminishes in importance relative to the 5f participation.

For a given actinide system, NPA populations indicate generally larger 5f and lower 6d population for O_h than for D_{3h} structures (or than for other low-symmetry stationary points in the case of UH_6). The larger 6d and lower 5f character of bonding in ThH_6^{2-} (Table 3) correlate with the preference for a D_{3h} structure. This is the only case where the d orbital involvement dominates the actinide hydride structure and thus renders it similar to the corresponding TM system (HfH_6^{2-}). In PaH_6^- and UH_6, the 5f orbitals are energetically lower and more compact, and they attain the predominant bonding role. The symmetry trend along the AnH_6^q series can thus indeed be ascribed to the growing structural influence of the 5f orbitals along the series, together with a constant influence of the d orbitals.

In his analysis of the AnO_2^q series, Dyall saw also an approximate constancy of 6d orbital participation in bonding and an increase of 5f participation with increasing nuclear charge of the metal.[6] He argued that the d orbitals can thus have no influence on the structural trends, and 5f/6d hybridization eventually favors the linear structures. While our results clearly support the role of the 5f orbitals in favoring the "classical" structures, it is obvious that the 6d orbitals dominate the structural preferences for the borderline case Th, before the f orbitals start to take over further along the series. It is important to note that while both d and f orbitals of a spherical atom span the full angular space, their energetical contributions to bonding in a molecule require specific symmetry behavior of individual orbitals participating in the most important frontier MOs. The *gerade* d orbitals favor low-symmetry structures without an inversion center[33,34] when involved only in σ-bonding,[14] whereas the *ungerade* nature of p and f orbitals[34] favors regular, "VSEPR-type" structures in main group and actinide chemistry, respectively.

The moderate 7s populations increase somewhat with increasing nuclear charge and are generally smaller for octahedral than for distorted structures (Table 3). The 7p orbitals appear generally too diffuse to play a decisive role in bonding. The role of the 6p semicore orbitals has been discussed previously in connection with a "6p sigma hole" in UO_2^{2+}.[2,6,9,10] NPA indicates a depopulation of actinide 6p semicore orbitals at the octahedral structures, particularly for UH_6. Due to the relatively isotropic bonding, the effect is comparatively small (0.1 electrons in UH_6 vs 0.5 electrons in UO_2^{2+}) but visible. It can be ascribed to repulsive polarization of the 6p shell by the ligand orbitals.

Table 4. Analysis of NAO Composition of NLMOs Corresponding to M−H Bonds in MH_6^q (M = Hf−W, Th−U) Complexes[a]

system	structure	metal NAO contribution (%)	metal NAO composition			
			s (%)	p (%)	d (%)	f (%)
HfH_6^{2-}	O_h	18.6	28.2	3.7	68.1	
	D_{3h}	22.2	22.5	2.4	75.1	
	C_{3v}	22.2	22.5	2.4	75.1	
TaH_6^-	O_h	23.9	26.1	2.7	71.3	
	D_{3h}	30.9	18.5	1.4	80.0	
	C_3	33.0	19.2	1.2	79.7	
WH_6	O_h	30.0	25.1	3.8	71.2	
	D_{3h}	40.7	16.3	1.5	82.2	
	C_{3v}	46.5	14.6	1.1	84.3	
	C_{3v}'	48.7	13.9	1.0	85.1	
	C_{5v}	46.3	12.7	1.1	86.2	
	C_{5v}'	51.1	12.2	0.8	87.3	
ThH_6^{2-}	O_h	11.0	44.1	1.7	30.9	23.3
		(10.7)	(43.9)	(0.6)	(55.6)	
	D_{3h}	10.9	40.5	0.6	45.4	13.5
		(10.6)	(43.8)	(0.6)	(55.6)	
PaH_6^-	O_h	22.4	24.3	4.7	10.2	60.8
		(11.9)	(51.7)	(3.5)	(44.7)	
	D_{3h}	21.0	22.4	1.1	17.9	58.7
		(13.5)	(42.2)	(1.3)	(56.5)	
UH_6	O_h	31.5	19.2	2.7	13.7	64.3
		(17.8)	(37.6)	(2.6)	(59.8)	
	D_{3h}	29.4	9.7	0.5	28.6	61.2
		(25.0)	(21.2)	(1.2)	(77.6)	
	C_{3v}	29.4	11.6	0.4	30.5	57.5
		(25.0)	(21.2)	(1.2)	(77.6)	
	C_{3v}'	31.1	12.0	0.8	38.2	49.2
		(26.4)	(18.3)	(1.7)	(80.0)	
	C_{5v}	30.2	13.7	0.4	35.6	50.4
		(24.7)	(21.2)	(1.1)	(77.8)	
	C_{5v}'	36.3	13.6	0.8	38.1	47.6
		(26.8)	(17.5)	(1.2)	(81.4)	

[a] Results for "d-only" actinides in parentheses. Data for lower-symmetry structures are averages over different positions.

NPA populations for "d-only" actinide systems indicate generally more ionic bonding than in the corresponding "true" actinide hydrides. The 6d population is enhanced upon removal of f functions from the basis set but cannot compensate completely the loss in 5f covalency. The 6d populations tend to be particularly large for the distorted, low-symmetry minima, analogous to the TM systems.

Table 4 shows analyses of natural localized molecular orbitals (NLMOs) for the M−H bonds (due to the choice of ionic NBO Lewis structures, the M−H bonds are expressed as hydrogen lone-pair NLMOs; see Computational Methods). These confirm the NPA results by exhibiting increasing 5f and decreasing 6d character along the actinide hydride series (with a particularly large step from ThH_6^{2-} to PaH_6^-), as well as more 6d and less 5f character in lower-symmetry structures compared to the octahedron. The "d-only" actinide calculations produce average d-character of the bonding NLMOs that is still a bit lower than that for the corresponding $5d^0$ TM complexes.

Table 4 provides only averages for all six M−H bonds of a complex. Tables S1 and S2 in the Supporting Information dissect NPA and NLMO data, respectively, into individual contributions from sites that are symmetrically inequivalent. The relations between covalency and bond lengths and bond angles in d^0 transition metal hexamethyl or hexahydride complexes have

(34) King, R. B. *Inorg. Chem.* **1992**, *31*, 1978.

Table 5. Calculated NPA Charges, Natural Atomic Populations, and Energies of Frontier Orbitals for MF_6^q (M = Hf−Re, Th−Np) Complexes[a]

system	structure	q(M)	q(F)	M(6p)	valence populations s	p	d	f	E_{HOMO} (au)	E_{LUMO} (au)	ΔE[b] (au)
HfF_6^{2-}	O_h	2.63	−0.77		0.20	0.02	1.15		−0.016 11	0.196 76	0.212 87
	D_{3h}	2.63	−0.77		0.19	0.02	1.16		−0.000 09	0.195 98	0.196 07
TaF_6^-	O_h	2.79	−0.63		0.24	0.02	1.95		−0.232 42	0.073 82	0.306 24
	D_{3h}	2.81	−0.63		0.24	0.02	1.94		−0.214 61	0.068 34	0.282 95
WF_6	O_h	2.57	−0.43		0.28	0.02	3.13		−0.469 68	−0.217 31	0.252 37
	D_{3h}	2.65	−0.44		0.28	0.02	3.10		−0.450 48	−0.219 62	0.230 86
ReF_6^+	O_h	2.45	−0.24		0.32	0.03	4.20		−0.719 32	−0.518 21	0.201 11
	D_{3h}	2.58	−0.26		0.32	0.03	4.10		−0.700 48	−0.522 60	0.177 88
ThF_6^{2-}	O_h	2.96	−0.83	5.98	0.10	0.01	0.25	0.69	−0.026 97	0.188 53	0.215 50
		(3.52)	(−0.92)	(6.00)	(0.12)	(0.02)	(0.34)		(−0.037 91)	(0.188 88)	(0.226 79)
	D_{3h}	2.99	−0.82	6.00	0.10	0.02	0.28	0.63	−0.013 38	0.188 14	0.201 52
		(3.50)	(−0.92)	(6.00)	(0.12)	(0.02)	(0.37)		(−0.023 00)	(0.188 84)	(0.211 84)
PaF_6^-	O_h	3.07	−0.68	5.95	0.11	0.01	0.21	1.64	−0.228 94	−0.015 25	0.213 69
		(4.36)	(−0.89)	(6.00)	(0.17)	(0.02)	(0.45)		(−0.242 20)	(0.088 43)	(0.330 63)
	D_{3h}	3.06	−0.68	5.97	0.10	0.01	0.24	1.62	−0.212 67	−0.018 53	0.194 14
		(4.33)	(−0.89)	(5.99)	(0.16)	(0.02)	(0.49)		(−0.226 19)	(0.081 66)	(0.307 85)
UF_6	O_h	3.05	−0.52	5.90	0.11	0.00	0.43	2.51	−0.443 28	−0.249 89	0.193 39
		(4.71)	(−0.78)	(6.00)	(0.17)	(0.03)	(1.10)		(−0.464 61)	(−0.184 33)	(0.280 28)
	D_{3h}	3.01	−0.50	5.94	0.10	0.01	0.48	2.46	−0.422 04	−0.249 66	0.172 38
		(4.67)	(−0.78)	(5.99)	(0.16)	(0.02)	(1.16)		(−0.448 67)	(−0.182 72)	(0.265 95)
NpF_6^+	O_h	2.90	−0.32	5.83	0.12	0.01	0.48	3.67	−0.682 13	−0.534 23	0.147 90
		(5.04)	(−0.67)	(6.00)	(0.20)	(0.03)	(1.73)		(−0.700 03)	(−0.463 25)	(0.236 78)
	D_{3h}	2.80	−0.30	5.90	0.10	0.01	0.52	3.68	−0.656 86	−0.526 80	0.130 06
		(5.01)	(−0.67)	(5.99)	(0.19)	(0.03)	(1.78)		(−0.684 34)	(−0.460 18)	(0.224 16)

[a] Results for "d-only" actinides in parentheses. [b] HOMO−LUMO gap.

been found previously to be rather complicated.[35] The corresponding trends for the "d-only" actinide hexahydride series follow closely those of the $5d^0$ complexes, suggesting again a remarkably close analogy in bonding.

We note in passing that the abovementioned instability of UH_6 toward H_2 elimination reflects probably the preference of uranium to maintain two electrons in pure nonbonding 5f orbitals, as hydrogen is not sufficiently electronegative to support strong covalent bonds. Moreover, the absence of any π-bonding also does not allow better stabilization of U^{VI} in this case. In contrast, the 5f shell is still sufficiently diffuse for Th or Pa.

Hexafluorides. In the case of TM d^0 systems, π-bonding tends to favor the octahedron in the MO picture by destabilizing the t_{2g} LUMO and thus disfavoring a second-order orbital mixing upon distortion.[14,16,29] This is the main reason the TM $5d^0$ hexafluorides prefer the octahedron (but with much smaller activation barriers for trigonal twist than in main group complexes[14]). Additionally, ligand repulsion tends to be enhanced compared to the hydrides, due to the somewhat larger bond ionicity (cf. Table 5). The increasing competitiveness of the trigonal prismatic transition state for trigonal twist along the TM series has been explained by increasing covalency in the σ-bonding framework (cf. hydride systems), decreasing ligand repulsion, and decreasing HOMO−LUMO gap. These arguments are confirmed by the NPA results for the TM hexafluoride systems in Table 5: Covalency increases along the $5d^0$ series, albeit somewhat less markedly than in the hexahydride series (cf. Table 3). Bonding in the hexafluoro complexes remains more polar than for the hydrides. The HOMO−LUMO gap at octahedral structures remains also much larger than for the hydrides (cf. Table 3).

In contrast to the hydrides, the trigonal prismatic transition state for the TM fluoro complexes is only slightly more ionic than the octahedral minimum. The NPA charges and atomic populations in O_h and D_{3h} structures are very similar. More information is gained by examining NLMOs (Table 6), as this allows us to distinguish between σ- and π-contributions (at least for the octahedral structures; σ-/π-separation of NLMOs remains incomplete for the D_{3h} structure). π-Bonding is already substantial for the TM hexafluoro complexes, with up to 11% metal 5d contribution to the formally fluorine π-lone-pair-type NLMOs in octahedral ReF_6^+. π-Bonding is clearly more efficient for the octahedron. In contrast, the NLMOs associated with the M−F σ-bonds tend to be more covalent (with more 5d and less 6s character) at the D_{3h} transition state than at the octahedral minimum. In agreement with previous work, these differences between σ- and π-bonding contributions at O_h and D_{3h} structures tend to increase along the $5d^0$ TM hexafluoro series.[14] Increasing stabilization of the prism by σ-bonding and decreasing ligand repulsion lead to the observed lowering of the activation barriers along the series.

Turning now to the actinide hexafluoro complexes (Tables 5,6), we note somewhat more ionic bonding than for the TM systems (cf. NPA charges, Table 5). The NLMO composition (Table 6) indicates that the covalency of both σ- and π-bonding components increases markedly from ThF_6^{2-} to NpF_6^+, but both remain less covalent than for the corresponding TM systems. The change in total charge of the complex from −2 to +1 is reflected mainly in reduced negative charge on the fluoride ligands. When looking at the NPA populations of individual angular momentum metal orbitals, we note that the 7s population remains small and almost constant (ca. 0.10 for O_h structures), the 7p population is almost negligible, and the 6d population is moderate and increases slightly. Most notably, the 5f population exceeds the 6d population already for ThF_6^{2-}, and it increases further dramatically along the series. As for the actinide hydrido complexes, a distortion of the octahedron increases the d population somewhat. In contrast, the 5f population is largest

(35) Kaupp, M. *Chem.—Eur. J.* **1999**, *4*, 1678.

Table 6. Analysis of NAO Composition of NLMOs Corresponding to Single M−F Bonds and Fluorine π Lone Pairs in MF_6[a] (M = Hf−Re, Th−Np) Complexes[a,b]

system	structure	NLMO	metal NAO contribution (%)	metal NAO composition s (%)	p (%)	d (%)	f (%)
HfF_6^{2-}	O_h	M−F	5.5	29.5	0.8	69.7	
		LP_π	2.7	0.0	2.5	97.5	
	D_{3h}	M−F	6.0	26.2	1.0	72.8	
		LP_π	2.5	0.1	3.1	96.8	
TaF_6^-	O_h	M−F	8.5	23.8	0.8	75.5	
		LP_π	4.8	0.0	1.0	99.0	
	D_{3h}	M−F	10.1	19.1	0.9	80.0	
		LP_π	3.9	0.0	1.4	98.6	
WF_6	O_h	M−F	12.4	18.8	0.8	80.4	
		LP_π	7.8	0.0	0.6	99.4	
	D_{3h}	M−F	15.7	14.2	0.7	85.1	
		LP_π	5.8	0.1	0.9	99.0	
ReF_6^+	O_h	M−F	15.6	17.1	0.9	82.0	
		LP_π	11.0	0.0	0.3	99.7	
	D_{3h}	M−F	21.1	12.0	0.7	87.3	
		LP_π	7.6	0.0	0.6	99.1	
ThF_6^{2-}	O_h	M−F	3.9	20.7	1.0	19.6	58.8
		LP_π	2.0	0.0	1.9	27.6	70.6
		(M−F)	(2.2)	(43.8)	(1.6)	(54.6)	
		(LP_π)	(0.9)	(0.0)	(8.6)	(91.4)	
	D_{3h}	M−F	3.6	20.6	1.7	30.7	47.1
		LP_π	2.0	0.0	2.6	23.5	73.9
		(M−F)	(2.6)	(33.1)	(1.9)	(65.1)	
		(LP_π)	(0.7)	(0.0)	(9.6)	(90.4)	
PaF_6^-	O_h	M−F	7.4	10.7	1.0	9.7	78.6
		LP_π	3.8	0.0	0.5	13.2	86.4
		(M−F)	(2.8)	(47.5)	(1.4)	(51.1)	
		(LP_π)	(1.2)	(0.0)	(6.3)	(93.7)	
	D_{3h}	M−F	6.4	10.5	0.8	14.6	74.0
		LP_π	4.4	0.0	0.8	10.6	88.6
		(M−F)	(3.3)	(36.4)	(1.3)	(62.3)	
		(LP_π)	(1.0)	(0.1)	(6.4)	(93.5)	
UF_6	O_h	M−F	13.2	5.4	3.0	11.2	80.5
		LP_π	5.7	0.0	0.5	17.9	81.6
		(M−F)	(4.5)	(26.3)	(1.0)	(72.7)	
		(LP_π)	(3.0)	(0.0)	(2.8)	(97.2)	
	D_{3h}	M−F	10.7	5.3	0.9	19.0	74.8
		LP_π	6.5	0.0	0.6	13.9	85.5
		(M−F)	(6.6)	(15.7)	(0.9)	(83.5)	
		(LP_π)	(2.1)	(0.1)	(3.2)	(96.7)	
NpF_6^+	O_h	M−F	19.3	3.5	2.5	8.7	85.3
		LP_π	7.8	0.0	0.7	14.7	84.6
		(M−F)	(6.2)	(22.6)	(1.0)	(76.4)	
		(LP_π)	(4.9)	(0.0)	(2.3)	(97.7)	
	D_{3h}	M−F	15.6	3.3	1.5	14.2	81.1
		LP_π	9.2	0.0	0.9	11.8	87.2
		(M−F)	(9.9)	(12.5	(1.2)	(86.4)	
		(LP_π)	(3.2)	(0.1)	(2.8)	(97.1)	

[a] Results for "d-only" actinides in parentheses.

for the octahedron, but differences are overall small (for NpF_6^+ the order is already reversed). It is thus clear that bonding involves again both 6d and 5f components, but with a large dominance of the latter.

Analysis of NLMOs for individual interactions (Table 6) provides more insight by separating σ- and π-bonding contributions. Upon distortion from O_h to D_{3h}, the σ-bonding NLMOs in the actinide hexafluoro complexes aquire more d character, as is the case for the TM d^0 systems. This is accompanied by a similarly substantial loss of 5f character. The latter dominates slightly, and thus the overall σ-covalency is reduced upon distortion, in contrast to the TM analogues. Things are just opposite for the π-bonding contributions. Here symmetry reduction from O_h to D_{3h} reduces the d and enhances the f character of a given NLMO (LP_π in Table 6). Except for ThF_6^{2-}, the earliest member of the series, the 5f contributions dominate again, and thus the overall covalent π-contributions are somewhat larger for the prismatic transition state. The overall structural preference is octahedral, meaning that the 5f contributions to σ-bonding prevail, assisted by 6d contributions to π-bonding and ligand repulsion.

Bonding in UF_6 as one of the most fundamental and important actinide complexes has been studied in great detail before.[15,36] Comparison of the highest occupied canonical MOs of octahedral WF_6, UF_6, and "d-only" UF_6 is nevertheless very instructive (Figure 4; only one component of triply degenerate sets is shown): The participation of the 5f orbitals in U−F bonding for "true" UF_6 is obvious, particularly for the t_{1u} and t_{2u} MOs.[15,36] While these 5f contributions are purely bonding in the lower t_{1u} level (HOMO-4) and in the t_{2u} orbital (HOMO-2), the second t_{1u} orbital is σ-bonding but π-antibonding and consequently becomes the HOMO.

In WF_6, as well as in "d-only" UF_6, these MOs are essentially ligand-centered nonbonding, as the *gerade* metal d orbitals cannot contribute to these *ungerade* MOs. The *ungerade* valence p orbitals (6p for WF_6 and 7p for UF_6) are energetically high-lying and diffuse. They contribute slightly to one of the t_{1u} MOs (Figure 4a,c), in the σ-bonding/π-antibonding manner described above for the 5f shell. As the p contribution is more pronounced for uranium, this MO is the HOMO-1 in "d-only" UF_6 but the HOMO-3 in WF_6. Both in WF_6 and in "d-only" UF_6, the HOMO has t_{1g} symmetry and is exclusively a ligand lone-pair combination. Overall, the electronic structure of the hypothetical "d-only" UF_6 resembles thus indeed remarkably that of its TM analogue WF_6.

For the prismatic transition states (cf. Figures S4 and S5 in the Supporting Information), the lower symmetry allows improved participation of the d orbitals in σ-bonding, increasingly so with increasing covalency along a given series, whereas the f orbitals are less suited for σ-bonding overlap in the prismatic structures. Matters are reverse for π-bonding.

4. Conclusions

Trends in the structural preferences of hexacoordinated actinide $6d^05f^0$ complexes differ from those of their previously studied transition metal homologues, mainly due to the dominance of the 5f orbitals in the former. Increasing 5f participation with increasing nuclear charge from ThH_6^{2-} to UH_6 causes a distinctly nonmonotonic structural change along the series. Relatively low f and significant d character of bonding in ThH_6^{2-} leads to a preference for a trigonal prism, analogous to the 5d homologue HfH_6^{2-}. Already with PaH_6^-, the octahedron prevails, but the structure becomes fluxional for UH_6. Unfortunately, uranium hexahydride is not a stable entity toward loss of H_2. Removal of f functions from the actinide basis set renders the structural preferences of the actinide hydrido complexes almost equivalent to those of their $5d^0$ analogues.

The octahedron dominates for the hexafluoro complexes, but the trend of activation barriers for trigonal twist via D_{3h} transition states is inverted for actinides: While the barriers decrease from HfF_6^{2-} to ReF_6^+, they increase significantly from ThF_6^{2-} to NpF_6^+. Again, removal of f functions from the actinide basis

(36) (a) Hay, P. J.; Wadt, W. R.; Kahn, L. R.; Raffenetti, R. C.; Phillips, D. H. *J. Chem. Phys.* **1979**, *71*, 1767. (b) de Jong, W. A.; Nieuwpoort, W. C. *Int. J. Quantum Chem.* **1996**, *58*, 203.

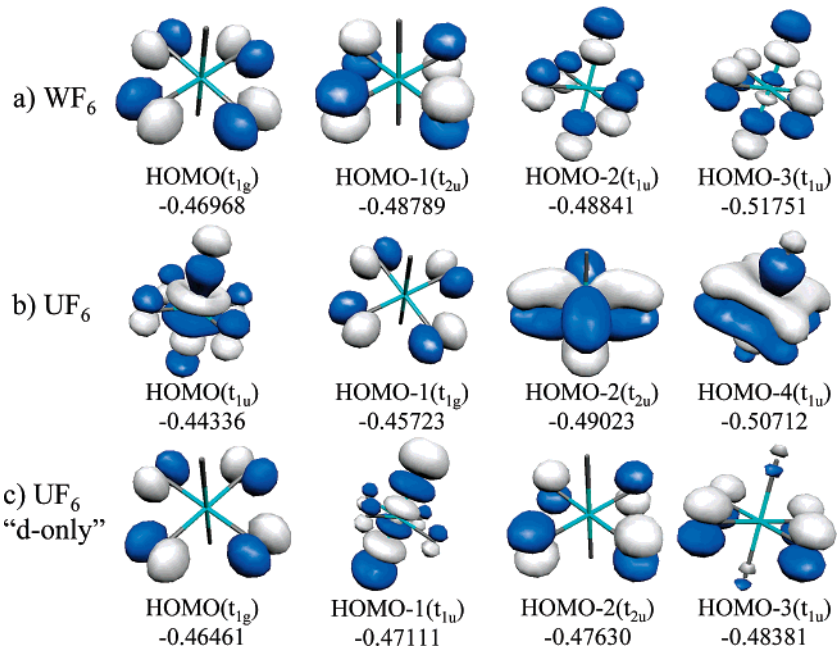

Figure 4. Highest occupied MOs of hexafluorides. (a) WF_6. (b) UF_6. (c) "d-only" UF_6 (the HOMO-3 in regular UF_6 is an a_{1g} MO[15] and has been omitted (cf. Figure S2 in Supporting Information); orbital energies in au).

sets reverts the trend, back to that of the transition metal analogues. Together with detailed bonding analyses, this corroborates the importance of the 5f orbitals for the structuraltrends of the $6d^05f^0$ species. Notably, the role that d and f orbitals play in σ- and π-bonding, respectively, appears to be just opposite in all cases. The *ungerade* nature of the f orbitals opens avenues of structure-bonding relationships that are not possible with only the *gerade* d orbitals.[34] In this sense, the influence of the f orbitals in actinide complexes restores to some extent main group structural preferences (dominated by the symmetry of the valence p orbitals) that are sometimes violated for d^0 systems,[14] due to the predominant influence of the valence d orbitals.

Acknowledgment. This work has been funded by Deutsche Forschungsgemeinschaft. Work in Bratislava has been supported by the Slovak Grant Agencies VEGA (No. 2/3103/23) and APVT (No. 51-045502), as well as COST D 18 action.

Supporting Information Available: Two tables (S1, S2) provide more detailed NPA and NLMO analysis data for hexahydride complexes. Five figures (S1−S5) provide a larger subset of canonical valence orbitals for octahedral and prismatic structures of UF_6 and WF_6. This material is available free of charge via the Internet at http://pubs.acs.org.

JA044982+